HAWAIIAN SKIRT: An F-Box Gene That Regulates Organ Fusion and Growth in Arabidopsis[1][C][W][OA]

Zinnia H. González-Carranza, Unchalee Rompa, Janny L. Peters, Anuj M. Bhatt, Carol Wagstaff, Anthony D. Stead, and Jeremy A. Roberts*

Plant Sciences Division, School of Biosciences, University of Nottingham, Sutton Bonington Campus, Loughborough, Leicestershire LE12 5RD, United Kingdom (Z.H.G.-C., U.R., J.A.R.); Section Plant Genetics, Institute for Wetland and Water Research, Radboud University Nijmegen, 6525 ED Nijmegen, The Netherlands (J.L.P); Department of Plant Sciences, University of Oxford, Oxford OX1 3RB, United Kingdom (A.M.B.); School of Biological Sciences, University of Southampton, Bassett Crescent East, Southampton S016 7PX, United Kingdom (C.W.); and School of Biological Sciences, Royal Holloway, University of London, Egham, Surrey TW20 0EX, United Kingdom (A.D.S.)

A fast neutron-mutagenized population of Arabidopsis (*Arabidopsis thaliana*) Columbia-0 wild-type plants was screened for floral phenotypes and a novel mutant, termed *hawaiian skirt* (*hws*), was identified that failed to shed its reproductive organs. The mutation is the consequence of a 28 bp deletion that introduces a premature amber termination codon into the open reading frame of a putative F-box protein (At3g61590). The most striking anatomical characteristic of *hws* plants is seen in flowers where individual sepals are fused along the lower part of their margins. Crossing of the abscission marker, Pro_{PGAZAT}:*β-glucuronidase*, into the mutant reveals that while floral organs are retained it is not the consequence of a failure of abscission zone cells to differentiate. Anatomical analysis indicates that the fusion of sepal margins precludes shedding even though abscission, albeit delayed, does occur. Spatial and temporal characterization, using Pro_{HWS}:*β-glucuronidase* or Pro_{HWS}:*green fluorescent protein* fusions, has identified *HWS* expression to be restricted to the stele and lateral root cap, cotyledonary margins, tip of the stigma, pollen, abscission zones, and developing seeds. Comparative phenotypic analyses performed on the *hws* mutant, Columbia-0 wild type, and Pro_{35S}:*HWS* ectopically expressing lines has revealed that loss of *HWS* results in greater growth of both aerial and below-ground organs while overexpressing the gene brings about a converse effect. These observations are consistent with HWS playing an important role in regulating plant growth and development.

Abscission involves the detachment of an organ from the body of a plant and takes place at a site that is predestined for the purpose (Sexton and Roberts, 1982; González-Carranza et al., 1998). The phenomenon may be triggered by a range of environmental stresses including drought, waterlogging, nutrient deficiency, or pathogen attack (Addicott, 1982; Taylor and Whitelaw, 2001), but is also programmed to occur at discrete stages during plant development such as after leaf senescence, flower fertilization, or fruit ripening have taken place. Although the precise events that bring about shedding are unclear the process is preceded by an increase in the activity of several wall-loosening enzymes including β-1-4 glucanase and polygalacturonase precisely at the site of abscission (Roberts et al., 2002). It is proposed that the action of these enzymes, coupled with an increase in expansin activity (Belfield et al., 2005; Sampedro and Cosgrove, 2005), may lead to the dissolution of the middle lamella that brings about cell separation (González-Carranza et al., 2002; Roberts et al., 2002).

To dissect further the mechanisms responsible for regulating the abscission process, forward genetic strategies have been employed to identify non- or delayed-shedding mutants followed by the mapping and characterization of the mutated genes (Patterson, 2001; Roberts et al., 2002). While a number of such mutants have been documented only a few of the genes responsible have been cloned and characterized. These include *jointless*, which is the consequence of a mutation in a MADS-box gene involved in the differentiation of abscission cells in the pedicel of tomato (*Solanum lycopersicum*) flowers (Mao et al., 2000), and *inflorescence deficient in abscission* where the mutated gene has been shown to encode a novel class of ligand that seems to play a key role both in defining the site of cell separation (Stenvik et al., 2006) and in regulating the final step of floral organ shedding in Arabidopsis (*Arabidopsis thaliana*; Butenko et al., 2003). Recently,

[1] This work was supported by a grant from the Biotechnology and Biological Sciences Research Council and a studentship funded by the government of Thailand.

* Corresponding author; e-mail jeremy.roberts@nottingham.ac.uk; fax 44–1159–516334.

The author responsible for distribution of materials integral to the findings presented in this article in accordance with the policy described in the Instructions for Authors (www.plantphysiol.org) is: Jeremy A. Roberts (jeremy.roberts@nottingham.ac.uk).

[C] Some figures in this article are displayed in color online but in black and white in the print edition.

[W] The online version of this article contains Web-only data.

[OA] Open Access articles can be viewed online without a subscription.

www.plantphysiol.org/cgi/doi/10.1104/pp.106.092288

quantitative trait loci analysis has led to the identification of a quantitative trait locus (*sh4*) that has played a critical role in the domestication of rice (*Oryza sativa*) by bringing about a reduced shattering phenotype (Li et al., 2006). Although the function of the gene is unknown its characteristics suggest that it acts as a transcription factor. Other genes that have been identified to contribute to the abscission process in Arabidopsis include: *HAESA* that encodes a Leu-rich receptor-like kinase (Jinn et al., 2000); *AGAMOUS-LIKE15*, a MADS-domain transcription factor that if nonfunctional results in a delay in the time course of abscission (Fernandez et al., 2000; Harding et al., 2003; Lehti-Shiu et al., 2005); and the redundant *BLADE ON PETIOLE1* (*BOP1*) and *BOP2* genes encoding two BTB/POZ domain proteins that when silenced result in a disruption in leaf patterning and floral organ abscission (Hepworth et al., 2005; Norberg et al., 2005).

During the screening of a fast neutron-mutagenized population of Arabidopsis Columbia-0 (Col-0) wild-type plants a mutant, termed *hawaiian skirt* (*hws*), was isolated that retained its floral organs even after silique desiccation had taken place. In addition to exhibiting a nonshedding phenotype *hws* also exhibited sepals that are fused for some distance along their margins. Other mutants from Arabidopsis that show varying degrees of sepal fusion include *unusual floral organs* (*ufo*) where the mutated gene has been shown to encode an F-box protein (Levin and Meyerowitz, 1995; Samach et al., 1999); *leafy*, which is the result of a mutation in a floral meristem identity gene (Schultz and Haughn, 1991; Weigel and Meyerowitz, 1993); and the *cup shaped cotyledon* (*cuc*) mutants (*cuc1*, *cuc2*, *cuc3*) that arise as a consequence of mutations in putative NAC-transcription factor genes (Aida et al., 1997; Takada et al., 2001; Vroemen et al., 2003). Interestingly, ectopic expression of the microRNA miR164, which has been shown to induce posttranscriptional down-regulation of *CUC1* and *CUC2* (Laufs et al., 2004), leads to the generation of flowers with fused sepals that fail to undergo the normal shedding process (Mallory et al., 2004). A number of other genes have been shown to play an important role in the specification of lateral organ boundaries in leaves or flowers including *LATERAL ORGAN BOUNDARIES* (Shuai et al., 2002), *LATERAL ORGAN JUNCTIONS* (Prasad et al., 2005), *PETAL LOSS* (Brewer et al., 2004), the *FUSED FLORAL ORGANS* (*FFO*) loci (*FFO1*, *FFO2*, *FFO3*; Levin et al., 1998), *HANABA TARANU* (Zhao et al., 2004), and *RABBIT EARS* (Krizek et al., 2006).

In this article, the mapping and identification of a mutation in a putative F-box gene (*At3g61590*), which is responsible for bringing about the *hws-1* phenotype, is described. Although the transcript of *HWS* accumulates throughout the plant, reporter gene analysis reveals that expression is restricted to only certain tissues. By comparing and contrasting the phenotypic features of *hws-1*, an overexpressing *HWS* line driven by the *35S* cauliflower mosaic virus (CaMV) promoter wild-type plants, a role for HWS in regulating plant growth and development has been highlighted.

RESULTS

Mutant Isolation and Characterization

The *hws-1* mutant was isolated, as a result of an inability to shed its floral organs, during a screen of M_2 progeny grown from a fast neutron-mutagenized population (dose: 55 Gy; Lehle seeds) of M_1 Arabidopsis seeds in the Col-0 (wild type) background. Sepals, petals, and anther filaments were retained throughout reproductive development and remained in situ even after silique desiccation and dehiscence had taken place. To study flower development in more detail material was harvested from positions throughout the primary inflorescence with the first being where petals were visible. From that position all subsequent flowers were numbered. A scanning electron microscope (SEM) study of *hws-1* flowers revealed that sepals of the mutant were fused, for a distance along the lower part of their margins, and that characteristically the sepal whorl was broader than that seen in wild-type plants (Fig. 1, A–F). While the shedding of petals and anther filaments did not take place in the mutant, fine structural analysis of these tissues indicated that abscission of these organs could be detected in both wild-type and *hws-1* flowers (Fig. 1, G–J). Cell separation at the sepal bases was also apparent in *hws-1* flowers, however, the timing of this was delayed in comparison to wild-type plants and the sepal whorl was retained even though abscised (Fig. 1, H and J).

Further SEM analysis revealed that no distinction could be made between the wild-type and *hws-1* plants during early bud development (Fig. 2, A, B, E, and F). However, by the time the buds have reached stage 10 (Smyth et al., 1990) the line of separation between individual sepals had become demarcated to the bud base in wild-type but not in *hws-1* material (Fig. 2, C and G). Initially the region of sepal confluence in *hws-1* is restricted to just a few cells; however, further division must take place so that by the time buds have reached stage 12 sepals are fused for nearly 25% of their distance (Fig. 2, D and H).

The *hws-1* mutant was crossed with a wild-type plant and a 3:1 segregation of shedding:nonshedding individuals in the F_2 population showed that the phenotype is due to a recessive mutation in a single gene of nuclear origin.

Crossing of an Abscission Zone-Specific Gene Marker into the *hws-1* Mutant

To determine whether the nonshedding phenotype of *hws-1* was due to a failure of abscission zone (AZ) differentiation a cross was made between the mutant and a transgenic marker line (Pro_{PGAZAT}:*GUS*) that expresses the reporter gene *GUS* specifically at the site of floral organ separation. *PGAZAT* (*At2g41850*) encodes a polygalacturonase that is transcribed immediately prior to organ abscission in Arabidopsis and is thought to contribute to cell wall degradation (González-Carranza et al., 2002). Several homozygous

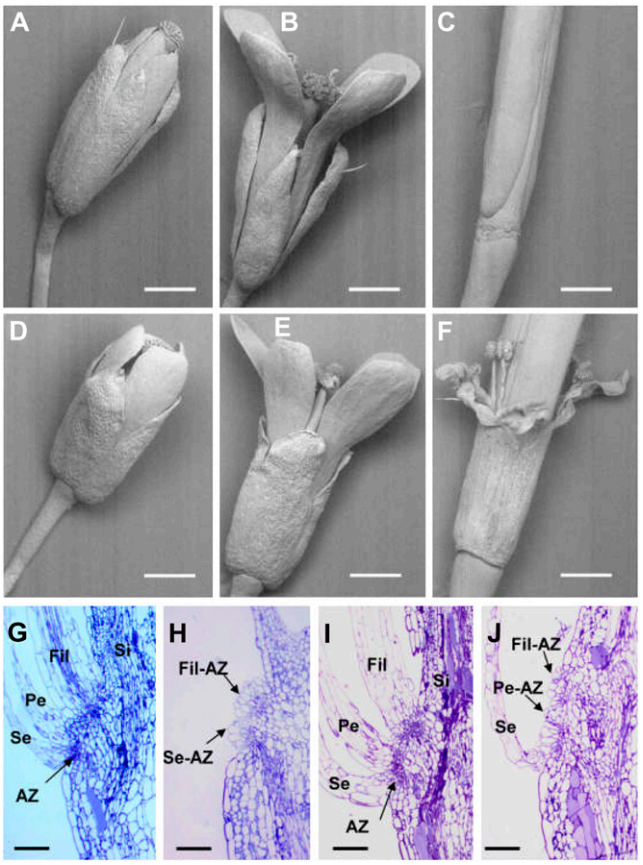

Figure 1. SEM and light microscope analyses of wild-type and *hws-1* flowers. Scanning electron microscopy of flower development stages in Col-0 wild type (A–C) and *hws-1* plants (D–F) at positions 2 (A and D), 6 (B and E), and 14 (C and F). Light microscopy of 5 μm longitudinal sections of flower AZs stained with Toluidine blue in Col-0 wild type (G and H) and *hws-1* plants (I and J) at position 4 (G and I), when petals (Pe) and sepals (Se) are still attached, and position 12 (H and J), when only sepals are attached to the *hws-1* mutant and siliques (Si) are visible at all stages. Sites of sepal (Se-AZ), petal (Pe-AZ), and anther filament (Fil-AZ) abscission are identified. Bars = 500 μm (A–F) and 50 μm (G–J). [See online article for color version of this figure.]

hws-1 lines containing the *GUS* gene were isolated. Figure 3, A and B, shows that both wild-type and mutant plants express the Pro_{PGAZAT}:*GUS* gene at the base of the sepals, petals, and anther filaments, indicating that the *hws* mutation does not seem to impede AZ differentiation. However, although Pro_{PGAZAT}:*GUS* expression is apparent in position 8 flowers of wild-type plants (Fig. 3A), it cannot be detected until position 10 in *hws-1* flowers (Fig. 3B). In addition, Pro_{PGAZAT}:*GUS* expression is less pronounced in *hws-1* plants and by position 20, in contrast to wild-type plants, expression of the reporter gene is no longer detectable at the site of floral organ abscission. For comparison, expression of Pro_{HWS}:*GUS* is shown at different positions throughout floral development (Fig. 3C). However, these observations will not be described in detail until a later part of the "Results" section of this article.

Other Phenotypic Features of the *hws* Mutant

The identification of another allele of *HWS* (*hws-2*) from the SALK collection (Alonso et al., 2003), during the course of mapping the gene, lead to the confirmation of additional phenotypic characteristics associated with the *hws-1* mutation.

A detailed analysis revealed that 28% of flowers in the *hws-1* mutant had fused anther filaments to differing extents along their length (Fig. 4A), compared with 2% in the wild type. Occasionally, in *hws-1* plants, these filaments were fused to the side of siliques (Fig. 4B). The top of the *hws-1* silique was consistently broader than wild type, and the length of the AZ region, exposed by manually removing the floral organs, was longer in the mutant (Fig. 4, C and D). Some *hws-1* siliques comprised more than two valves (Fig. 4E) and dissection of aberrant pods revealed that this was associated with abnormal development of the septum (Fig. 4F). The lamina tissue of the primary cauline leaves of *hws-1* plants routinely exhibited fusion to the inflorescence stems (Fig. 4G).

Mapping the *hws* Locus

Homozygous *hws-1* (Col-0 ecotype) plants were crossed with the Landsberg *erecta* (L*er*) ecotype and the F_2 progeny used as a mapping population. An amplified fragment length polymorphism (AFLP)-based genome-wide approach (Peters et al., 2004) was adopted to map the *hws* mutation to a 3.28 Mb domain at the bottom of chromosome 3. Using cleaved amplified polymorphic sequences (CAPS), simple sequence length polymorphisms (SSLPs), and insertion/deletion (InDel) markers this interval was reduced to a region of 56 kb containing 18 annotated genes (Fig. 5A).

Insertional mutant lines from the SALK collection of these 18 candidate genes were examined and two individuals in a population of 50 plants from line SALK_088349 (located in the gene *At3g61590*) exhibited phenotypic characteristics reminiscent of *hws-1*. Further analysis of this line revealed that it contained two T-DNA insertions, arranged in opposing configurations, downstream from the ATG of the *At3g61590* gene. These insertions were located 475 and 491 bp from the ATG (Fig. 5B).

PCR amplification of the *At3g61590* genomic region of wild type and *hws-1* DNA and restriction analyses of the amplified products with the high frequency cutting enzymes *Alu*I, *Rsa*I, and *Taq*I revealed subtle differences in banding patterns between the two genotypes (Fig. 5C). Sequencing of this region from *hws-1* revealed that it contained a 28 bp deletion located 966 bp downstream of the translation start of the open reading frame (ORF) of *At3g61590*. The consequence of this deletion is to introduce a frame shift resulting in the introduction of a premature termination amber codon in place of an Ile residue and the predicted production of a truncated version of the At3g61590 protein (Fig. 5B).

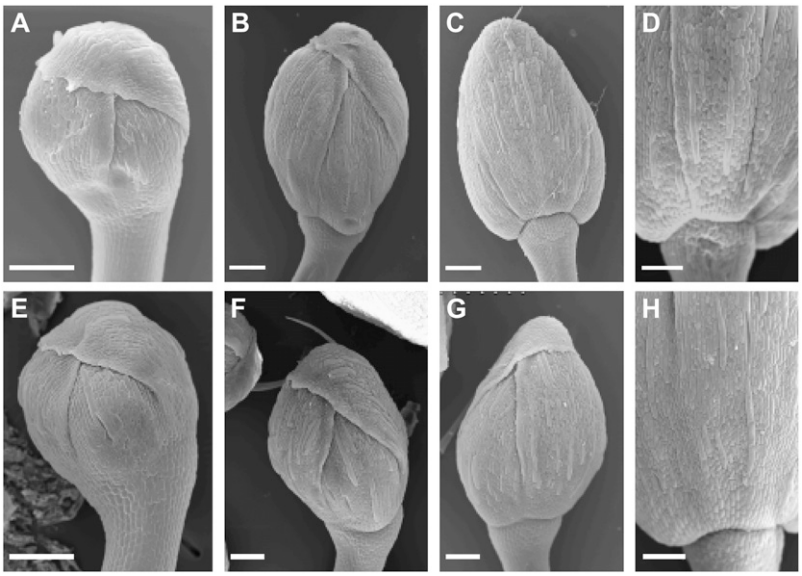

Figure 2. SEM analysis of wild-type and *hws-1* buds at developmental stage 6 (A and E), stage 8 (B and F), stage 10 (C and G), and stage 12 (D and H). Buds dissected from Col-0 wild type (A–D) and *hws-1* (E–H) plants. Bars = 100 μm.

To determine whether the *hws-1* phenotype was a consequence of a mutation in the *At3g61590* gene, a cross between the mutant and the SALK_088349 line (knockout [KO]) was performed. All progeny of this cross displayed *hws-1* characteristics. To test that these had not arisen by a self-pollination event two plants were analyzed by PCR and reverse transcription (RT)-PCR. The PCR demonstrated that both a gene-specific product (originating from the *hws-1* mutant) and an insertion product (originating from the KO) were amplified in each individual but only the former was present in the wild-type control (Fig. 5D). RT-PCR analysis of RNA extracted from various tissues of the SALK_088349 line and from two F_1 plants (*hws-1* × KO) showed no *At3g61590* expression in the KO but the presence of a transcript in both progeny (Fig. 5E).

Proof that *HWS* is encoded by the *At3g61590* gene was obtained by complementing the *hws-1* mutant with a 3.513 kb fragment amplified from wild-type DNA containing 1,291 bp upstream of the promoter, plus the 5′ and 3′ untranslated regions (UTRs), and intron and exon of the *At3g61590* gene. This segment proved to be of sufficient length to rescue fully the *hws-1* mutant (Fig. 5F).

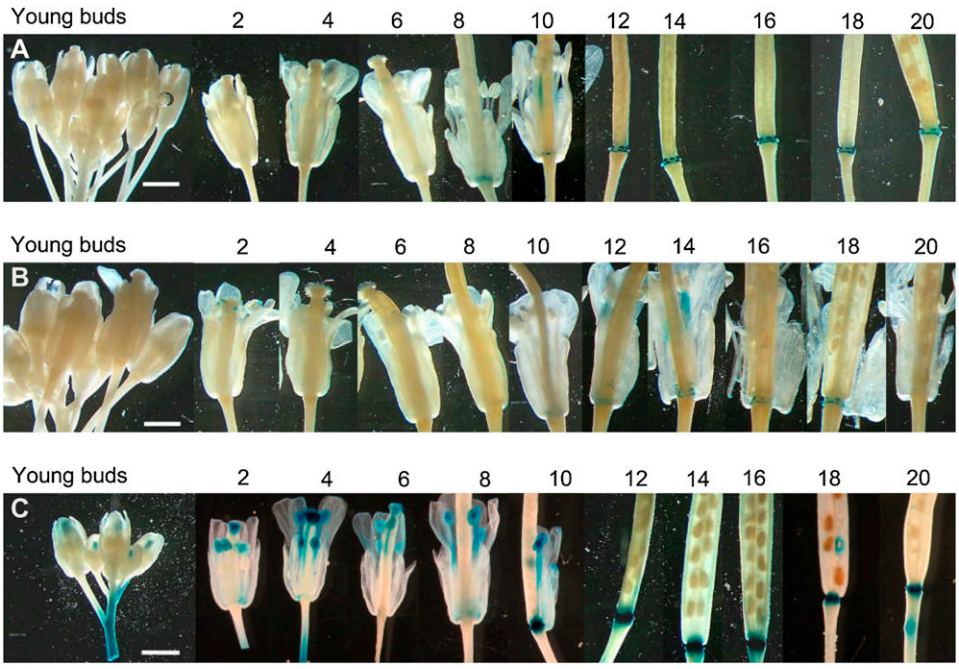

Figure 3. Flower and silique expression from Pro_{PGAZAT}:*GUS*, Pro_{PGAZAT}:*GUS* crossed into *hws-1*, and Pro_{HWS}:*GUS*. Time course of expression from different developmental positions of flower and siliques of GUS-stained tissue after 12 h incubation in GUS substrate. Flowers are identified from positions 2 to 20. Position 1 is the first flower where petals are visible to the eye. A, Pro_{PGAZAT}:*GUS*. B, Pro_{PGAZAT}:*GUS* crossed into *hws-1*. C, Pro_{HWS}:*GUS*. Bars = 1 mm.

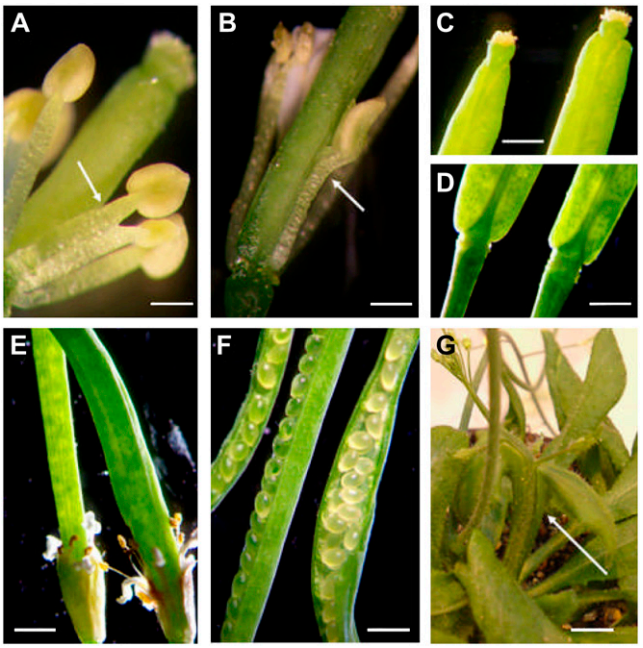

Figure 4. Phenotypic characteristics of *hws-1*. Characteristics shown in C, D, and G appeared consistently. A, Fused anthers (arrow). B, Anther fused to the silique (arrow). C, Top of mature silique from Col-0 wild type (left) or *hws-1* (right). Note the difference in width of silique and length of residual papillae. D, Bottom of mature silique from Col-0 wild type (left) or *hws-1* (right). Note the difference in longitudinal dimensions of the AZ region. E, Siliques from *hws-1* with more than two valves. F, Dissected siliques from Col-0 wild type (left and center) and *hws-1* (right) with aberrant septum development. G, First cauline leaves from *hws-1* fused to the stem of the inflorescence (indicated by an arrow). Bars = 500 μm (A–F) and 5 mm (G). [See online article for color version of this figure.]

HWS Encodes a Putative F-Box Protein

The likely function of the *HWS* gene (*At3g61590*) is that it encodes an F-box protein. These proteins, as part of a SCF complex, are proposed to interact with a substrate leading to their degradation by the 26S proteasome (Ni et al., 2004). *HWS* encodes a protein of 412 amino acids. It has no introns within the ORF but has an intron of 532 bp within the 5′ UTR of the gene (Fig. 5B). The truncated version of the mutant protein, predicted to be generated in *hws-1* plants, contains the intact F-box region. Information retrieved from the Web site PlantsUBQ, which is a functional genomics database for the Ubiquitin/26S proteasome proteolytic pathway in plants (http://plantsubq.genomics.purdue.edu/plantsubq/cgi-bin/detail.cgi?db=plantsubq&id=163137), indicates that the predicted F-box domain of HWS is located between amino acids 40 and 85. The software also proposes the existence of a transmembrane-spanning region between amino acids 120 and 140 and a low similarity (29.3%) to a Kelch_2 motif in the region between amino acids 290 and 338.

Outside the F-box region, the ORF of *HWS* shows only a low level of sequence similarity with other putative F-box proteins that have been annotated within the Arabidopsis genome. The Arabidopsis gene encoding a protein with highest sequence similarity (approximately 30%) to HWS is *UFO*. UFO is a protein that has been shown to be required for normal patterning and growth of the floral meristem (Samach et al., 1999).

Spatial and Temporal Expression of the *HWS* Gene

RT-PCR analysis of RNA isolated from wild-type plants revealed that the *HWS* transcript is expressed in many different tissues of the plant. Levels of expression were highest in buds and flowers, however, expression could also be detected in roots, leaves, stem, and siliques (Fig. 6). A more detailed analysis of the spatial and temporal pattern of expression, with the aid of the *GUS* or *green fluorescent protein* (*GFP*) reporter genes fused to the *HWS* promoter, showed that the gene is expressed at discrete sites within a range of tissues including the outer margins of cotyledons (Fig. 7A), the sepals of young buds and flowers (Fig. 7, B–D), the stigmatic papillae and tip of the elongating silique (Fig. 7, E and G), the base and vascular tissue of petals and sepals (Fig. 7F), the anther filaments and pollen (Fig. 7G), the floral and cauline leaf AZs (Fig. 7, H and I), the testa of developing seeds (Fig. 7J), the vascular tissue of the primary root and emerging laterals (Fig. 7K), and lateral root cap (Fig. 7L). A detailed time course of GUS accumulation during flower and silique development revealed that intense *HWS* expression could be detected at the site of floral organ abscission in position 8 flowers continuing up to the stage when desiccation of the pods took place (Fig. 3C).

Ectopic Expression of the *HWS* Gene Produces Smaller Seedlings

Transgenic plants were generated where the ORF from the *HWS* gene was expressed ectopically using a double *35S* CaMV promoter. Homozygous plants from two lines (8.3, A23.3) were examined in detail as RT-PCR analysis had indicated that these lines most strongly expressed both *HWS* and the transgene (Supplemental Fig. S1) and contained only a single insertion (data not shown).

Line 8.3 exhibited a more severe phenotype than line A23.3 in all the experiments that were undertaken. A growth study, carried out 2 weeks after emergence, revealed that both ectopic expressing lines were substantially smaller than wild type (Fig. 8A). However, *hws-1* plants at the same stage were larger than the control (Fig. 8A). Compared to the wild type, the rosette leaves of the overexpressing lines had shorter petioles, narrower and more rounded lamina with serrated borders, and displayed a greater degree of hyponastic bending (Fig. 8B).

Impact of Ectopic Expression of *HWS* on Flower Development

A comparison of flower development in wild type, *hws-1*, and Pro_{35S}:*HWS* line 8.3 demonstrated that

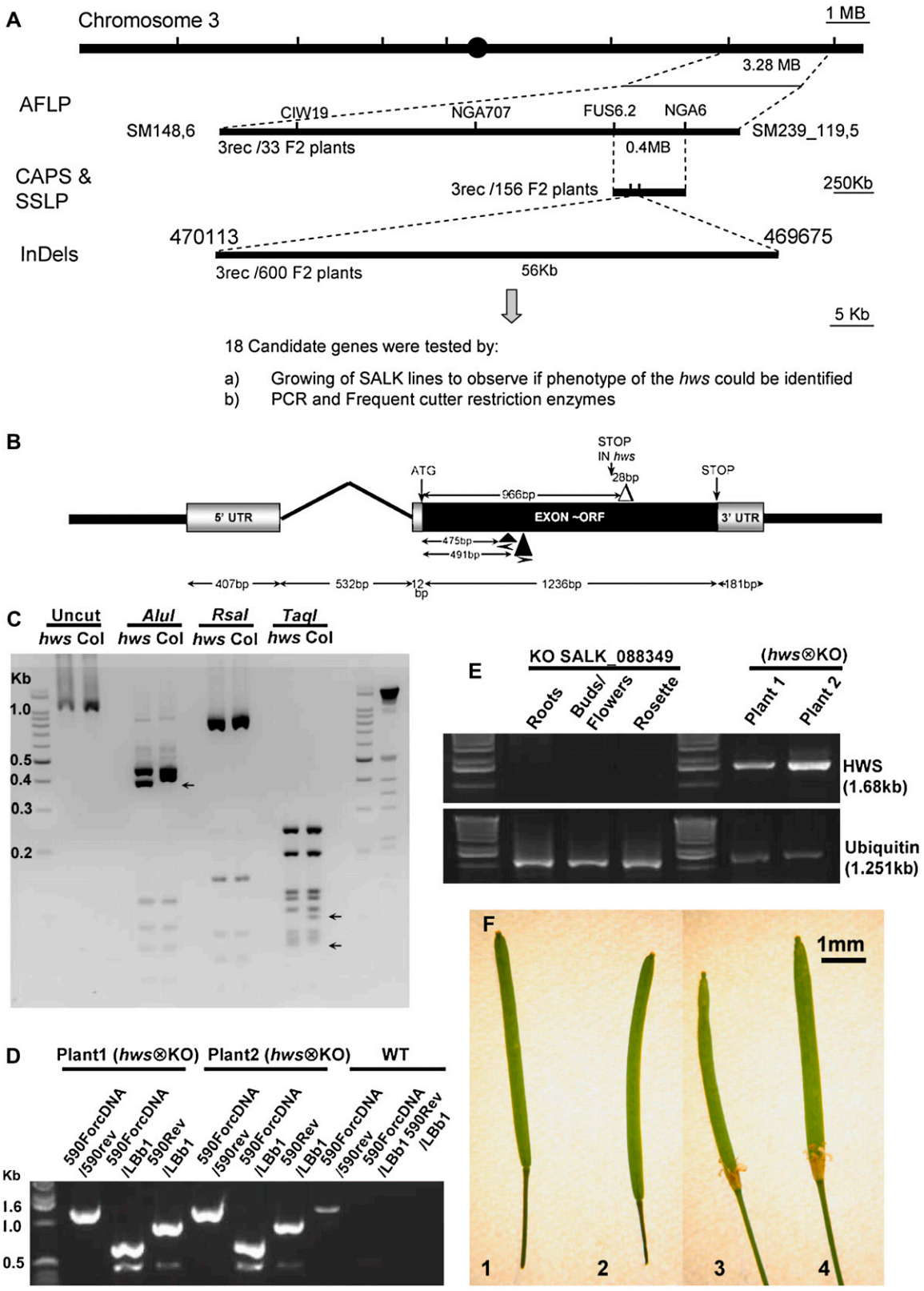

Figure 5. Mapping and identification of the *HWS* gene. A, Mapping strategy used to identify the *HWS* locus using an AFLP approach to analyze the DNA from 33 F_2 *hws-1* mutant plants. The initial location of the locus was identified to a region of 3.28 MB at the bottom of chromosome 3 between the markers SM148,6 and SM239_119,5. Further use of CAPS and SSLP on DNA from 156 F_2 *hws-1* mutant plants allowed the reduction of the region to a segment of 0.4 MB. With the use of InDels on DNA from

organ shedding took place at an earlier developmental stage in the overexpressing line (position 10) compared to the wild type (position 12). Flowers from line 8.3 also underwent sepal senescence prematurely, as evidenced by a visual decline in chlorophyll, compared to the wild type (Fig. 9; Supplemental Fig. S2). Figure 9 shows that *hws-1* had the longest, while the overexpressing line had the shortest, stigmatic papillae. A close-up view of flowers confirmed these observations (Supplemental Fig. S2).

Measurements of dissected sepals and petals from flowers at position 3 revealed that *hws-1* had significantly longer and wider sepals and petals compared to the wild type or Pro_{35S}:*HWS A23.3* line. The floral bases of the two overexpressing lines were the narrowest (Fig. 9; Supplemental Fig. S3), while *hws-1* was the widest compared to the wild type (see also Fig. 1, B and E).

Manipulation of *HWS* Expression Affects Root Growth and Seed Size

Seeds from *hws-1*, wild type, and the two overexpressing lines were germinated in germination medium (GM) or Murashige and Skoog media and root length was measured after a period of 2 weeks. The mutant exhibited the longest roots while both Pro_{35S}:*HWS* lines 8.3 and A23.3 had significantly shorter roots than the wild type (Fig. 10A).

The dimensions of mature seeds from the three different genotypes were analyzed. The *hws-1* mutant was found to have statistically larger (both in length and width) seeds compared to the wild type while the overexpressing lines produced the smallest seeds (Fig. 10B).

DISCUSSION

We have described the isolation and characterization of a novel Arabidopsis mutant termed *hws* that fails to shed its floral organs. The mutated gene responsible for bringing about this phenotype (*At3g61590*) encodes a putative F-box protein. *HWS* is expressed throughout the plant but reporter gene analysis indicates that expression is restricted to specific tissues. Loss of *HWS* function results in an elevation of plant size while overexpression of the gene, using the *35S* CaMV promoter, generates plants exhibiting a significant reduction in root and vegetative shoot growth. These observations are consistent with HWS playing a role in the regulation of organ development in Arabidopsis.

Phenotype of the *hws* Mutant

The *hws-1* mutant was originally isolated as a consequence of an inability to shed its sepals, petals, and anther filaments. Indeed, these organs are retained throughout silique growth and development and remain at the base of the silique even after desiccation and dehiscence is complete. A close examination of the flowers has revealed that the mutation results in the fusion of the sepals along their basal margins. Ectopic expression of the microRNA *miR164* results in the generation of flowers with similar characteristics (Mallory et al., 2004). This miRNA is thought to act by targeting for degradation the mRNA of the genes *CUC1* and *CUC2* (Laufs et al., 2004). In addition to exhibiting fused sepals, *hws-1* has a prevalence to generate fused anthers, multivalved first-formed siliques, and fusion of the cauline leaf lamina to the inflorescence stem. These observations suggest that, like *CUC1* and *CUC2*, the *HWS* gene might act to regulate lateral boundary development and that the degree of penetrance of some of its phenotypic characteristics could be due, in part, to redundancy between HWS and other peptides.

An examination of the early stages of development in wild-type and *hws-1* plants indicates that floral morphology is initially indistinguishable, however, while sepal separation proceeds to the base of the bud in wild type this is terminated prematurely in *hws-1* material. Thus the *hws* phenotype is not the consequence of postgenital fusion of the sepals but due to their failure to undergo complete separation.

Figure 5. (*Continued.*)
600 F_2 *hws-1* plants, the region was reduced to a 56 kb segment between InDel 470113 and 469675. This region contained 18 candidate genes. Insertional SALK lines of these 18 genes were analyzed for *hws-1* characteristics and the DNA from region *At3g61590* was amplified by PCR and products were subject to digestion by restriction enzymes. B, Structure of the *HWS* gene. The gene has a 5′ UTR of 419 bp interrupted by an intron of 532 bp, an ORF of 1,236 bp, and a 3′ UTR of 181 bp. The *hws-1* mutation is a consequence of a 28 bp deletion 966 bp downstream from the ATG that introduces a premature amber nonsense codon. Individuals from the SALK_088349 line (*hws-2*) that phenocopies the *hws-1* mutation have two T-DNA insertions inserted in opposite directions 475 and 491 bp downstream from the ATG (shown). C, Patterns of digestion with frequent cutters *Alu*I, *Rsa*I, and *Taq*I from the region corresponding to the position of gene *At3g61590*. Arrows indicate different patterns of digestion between the *hws-1* mutant and the Col-0 wild type. D, PCR in two progeny plants from the *hws-1* mutant and the SALK_088349 line (*hws-2*) and the Col-0 wild type with insert primers and specific primers; note that two bands were amplified with vector border primer and each one of the specific primers, indicating that this line has two insertions. E, RT-PCR in root, bud/flower, and rosette tissues from the SALK_088349 line (*hws-2*) and a mix of the same tissues in two progeny plants from the *hws-1* mutant and SALK_088349 (*hws-2*). Ubiquitin (At4g05320) primers were used to demonstrate equal amounts of mRNA amplified. F, Complementation of *hws-1* using a 3.5 kb genomic fragment including the promoter, UTRs, intron, and exon of *At3g61590*. Siliques from position 16: (1) Col-0 wild type, (2) F_1 complementation plants, (3) *hws-1* mutant, and (4) SALK_088349 KO line (*hws-2*). [See online article for color version of this figure.]

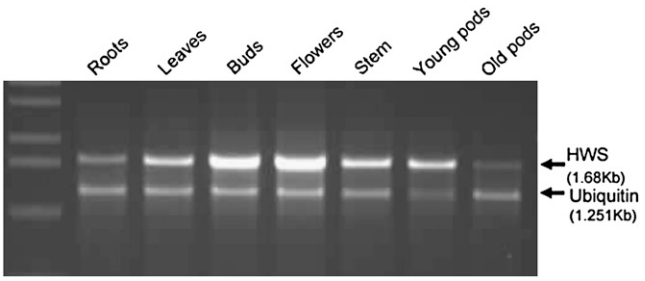

Figure 6. Analysis of expression of the *HWS* gene by RT-PCR. RT-PCR of RNA extracted from Arabidopsis Col-0 wild-type tissues using *HWS* or ubiquitin (At4g05320) primers.

To test whether differentiation of the floral AZs was taking place in *hws-1* we crossed the gene marker Pro_{PGAZAT}:*GUS* into the mutant. *PGAZAT* (*At2g41850*) encodes a polygalacturonase that is expressed specifically within the AZ cells of Arabidopsis and has been proposed to play a role in middle lamella degradation (González-Carranza et al., 2002). The results show that *hws-1* is not compromised in terms of AZ differentiation, however, the onset and duration of Pro_{PGAZAT}:*GUS* expression is delayed and reduced, respectively, in the mutant. These revelations, together with our SEM and light microscope observations, indicate that the nonshedding phenotype of *hws-1* is not the consequence of a failure of cell separation to take place at the base of petals, anther filaments, and sepals. While the fusion of the sepal margins, encircling the separated petals and anthers, provides a structural barrier to preclude organ shedding in *hws-1* our data indicate that the timing of cell separation in the mutant is delayed.

HWS Gene Encodes an F-Box Protein

Mapping and characterization of the *hws-1* locus has revealed that the mutant phenotype is a consequence of a 28 bp deletion in the ORF of a gene (*At3g61590*) encoding a putative F-box protein. The 28 bp deletion in *hws-1* introduces a premature translation termination codon, predicted to truncate HWS. The phenotype of *hws-1* is indistinguishable from that of a null mutant (SALK_088349; *hws-2*) caused by the insertion of two T-DNAs into *At3g61590*, suggesting that the shortened HWS protein, if synthesized, is nonfunctional. Evidence to support the proposal that HWS functions as an F-box protein has come from the demonstration by Takahashi et al. (2004) that in a targeted yeast (*Saccharomyces cerevisiae*) two-hybrid screen At3g61590 strongly associates with a number of Arabidopsis Skp1-related proteins (ASKs). We have confirmed that HWS interacts with both ASK1 and ASK4 in an anther-specific yeast two-hybrid library (X. Zhang, Z.H. González-Carranza, and J.A. Roberts, unpublished data).

HWS contains a single intron located within the 5′ UTR region of the gene. A bioinformatic analysis of HWS indicates that in addition to having an F-box domain, the protein contains a predicted transmembrane sequence, and a Kelch-like repeat region. The truncated protein produced by the *hws-1* mutant would lack an important element of the Kelch_2 motif and it has been proposed that this region, in other F-box proteins, might play a key role in the recognition of the substrate (Jarillo et al., 2001). It is possible therefore that the abbreviated version of HWS might have the capacity to bind ASKs but not the peptide targeted for degradation. Over 700 annotated genes within the genome of Arabidopsis have been classified,

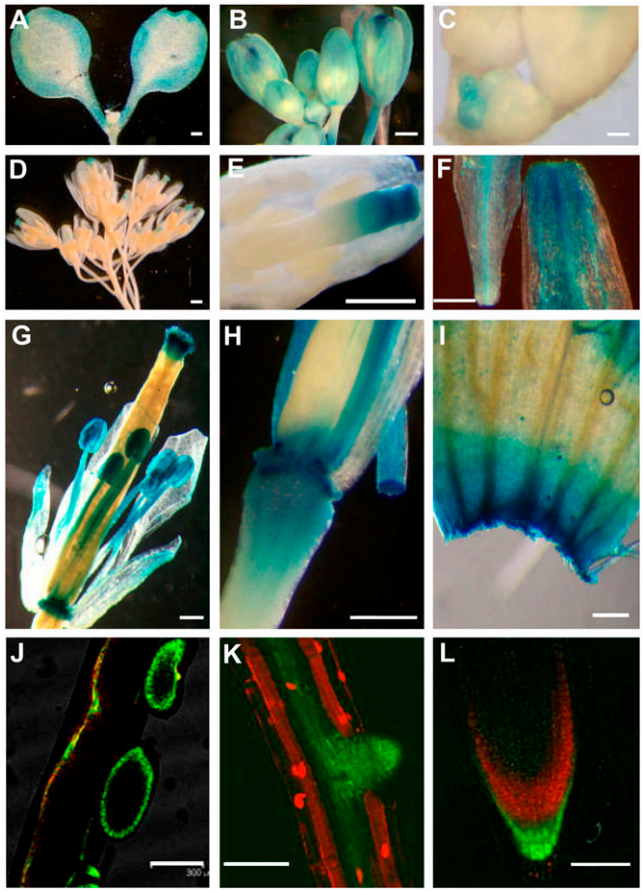

Figure 7. Analysis of expression from Pro_{HWS}:*GUS* and Pro_{HWS}:*GFP* transgenic lines. Cleared whole-mount GUS-stained tissue samples after 12 h from Pro_{HWS}:*GUS* plants at different stages of development (A–I) and confocal images from plant Pro_{HWS}:*GFP* (J–L). A, Two-day-old seedling. B, Young flowers (note the GUS expression in sepals including their vascular tissue). C, Close view of youngest floral buds. D, Young buds (note GUS expression becoming more discrete at the top of the silique as the flowers become older). E, Close view of the silique from a flower where petals have not emerged (note that GUS expression is spread along approximately one-third of the top of the silique). F, Separated petal (left) and sepal (right) material from a position 12 flower. G, A flower from position 9 (note how the GUS expression from the top of the silique becomes more localized at the stigma). H, An AZ from a flower of position 10. I, An AZ from a cauline leaf. J, A confocal image of developing seeds isolated from a mature silique. K, A confocal image of an emerging lateral root. L, A confocal image of a root cap. Bars = 300 μm (A, B, and D–K) and 75 μm (C and L).

Figure 8. Comparative phenotypic analysis of young plants. Two-week-old plants were analyzed and compared from: (1) Pro_{35S}:*HWS* homozygous line 8.3, (2) *hws-1*, (3) Col-0 wild type, and (4) Pro_{35S}:*HWS* homozygous line A23.3. A, A comparison of 2-week-old plants. B, Plants from A dissected to show size, shape, and number of leaves and cotyledons. Images of the remaining plantlets are on the far right. Bars = 5 mm. [See online article for color version of this figure.]

on the basis of sequence similarity, to be members of the F-box super family. The ORF of HWS shows only a low level of sequence similarity to other family members with the highest (approximately 30%) being to that encoded by the *UFO* gene. UFO has been shown to have a role in several aspects of flower development. Mutations in the *UFO* gene can bring about inappropriately fused floral organs (Levin and Meyerowitz, 1995) through its role in regulating patterning of primordial initiation. In addition, UFO is required for the specification of organ identity through its ability to promote the function of the type B class of floral homeotic genes (Durfee et al., 2003) and, by conditionally restoring UFO function, an additional role for the protein in regulating petal outgrowth has been identified (Laufs et al., 2003). There is no evidence that HWS plays a role in specifying organ identity as neither alleles of the *hws* mutant, that we have examined, show consistent evidence of abnormalities in floral organ identity. In addition, it is evident that HWS functions within vegetative tissues and that, if silenced, results in fusions of tissues such as the cauline leaf lamina to the stem of the inflorescence.

Expression of *HWS*

As the phenotypic characteristics of the *hws-1* mutant were primarily restricted to the shoot and reproductive tissues it was a surprise to discover that the transcript of the *HWS* gene could be detected by RT-PCR at high levels throughout the plant. Reporter gene analysis, using either GUS or GFP, revealed that although expression is evident in many tissues *HWS* promoter activity is restricted to specific cell types or regions of an organ. In roots, the pattern of expression is limited to the vascular tissues and the cells that comprise the lateral root cap. In leaves and stems expression is rarely detected in the vasculature but is associated with the margins of cotyledons. Floral tissues strongly express HWS with GUS activity being detected throughout development in sepals, the distal

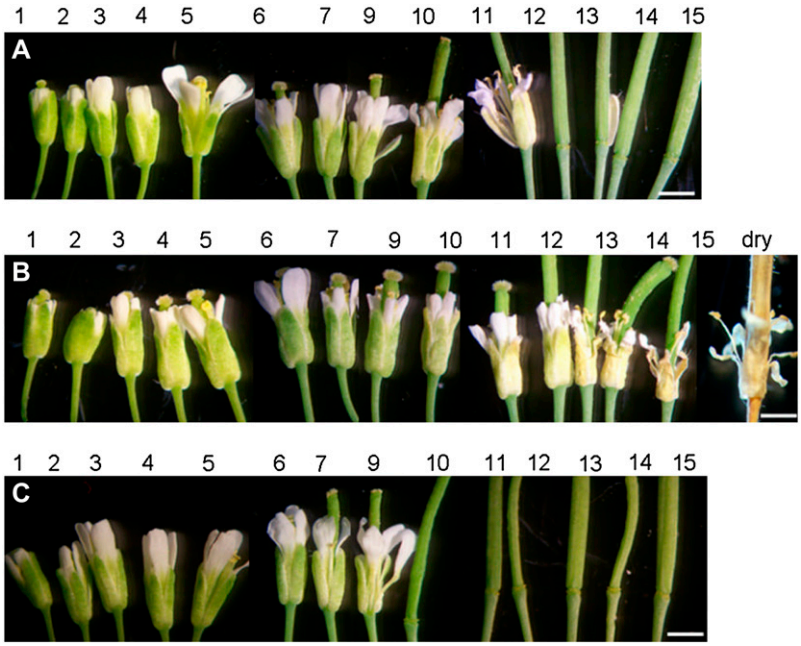

Figure 9. Comparative phenotypic analysis of flowers. Flowers of 4-week-old plants were analyzed and compared. The flowers are identified from position 1 to 15, considering position 1 as the first flower where petals are visible to the eye, and in the *hws-1* mutant a dry silique was included to show the presence of floral organs at that late stage of development. A, Col-0 wild type. B, *hws-1* mutant; note the bigger stigmatic papillae in the flowers and wider floral bases. C, Pro_{35S}:*HWS* line 8.3; note that abscission takes place earlier (position 10) than in the Col-0 wild type (position 12). Bars = 1 mm. [See online article for color version of this figure.]

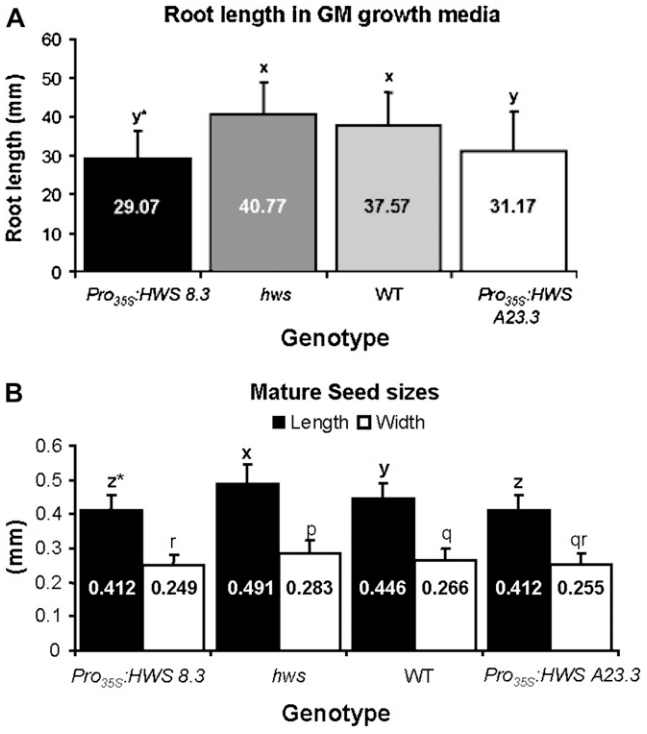

Figure 10. Comparative phenotypic analysis of root length and seed size. A, Twenty-six roots from 2-week-old seedlings grown in GM were photographed and their roots measured and statistically analyzed. Root length comparisons among Pro_{35S}:*HWS* line 8.3, *hws-1* mutant, Col-0 wild type, and Pro_{35S}:*HWS* line A23.3. The significance was analyzed by ANOVA test. *, Different characters (x, y) indicate a significant difference in the mean at $P < 0.05$, $n = 26$. B, Seventy dry seeds from five independent plants were photographed, measured, and statistically analyzed. Seed length and width comparisons among Pro_{35S}:*HWS* line 8.3, *hws-1* mutant, Col-0 wild type, and Pro_{35S}:*HWS* line A23.3. The significance of the differences was analyzed by ANOVA test. *, Different characters (p, q, r and x, y, z) indicate a significant difference in the mean at $P < 0.05$, $n = 70$.

end of the stigma, anther filaments, and pollen. Expression is also evident in the AZs of cauline leaves and floral organs. Aspects of the root and floral organ expression pattern are reminiscent of that exhibited by the F-box protein TIR1 (Gray et al., 1999) that has been shown to encode a receptor for indole-3-acetic acid (Kepinski and Leyser, 2005). Mutations in the *TIR1* gene confer a reduced sensitivity to indole-3-acetic acid, however, the responses of *hws-1* to auxin are indistinguishable from wild-type plants (Z.H. González-Carranza and J.A. Roberts, unpublished data) and while ectopic expressing lines of *HWS* exhibit reduced root growth, elongation of laterals root is not promoted.

GUS expression in Pro_{HWS}:*GUS* plants is intense at both the site of abscission of floral organs and cauline leaves. Expression precedes sepal, petal, and anther filament shedding and is maintained throughout silique development and maturation. This spatial and temporal pattern of expression is similar to that observed by genes that have been proposed to contribute to the process of cell separation (González-Carranza et al., 2002). Although anatomical analysis indicates that floral organ shedding is precluded by fusion of the sepals in *hws* plants, rather than as a consequence of a failure to undergo cell separation, a comparison between the mutant, overexpressing lines and wild-type plants demonstrates that HWS does, in addition, have a direct influence on the timing of abscission. A study of the mutant material crossed with the Pro_{PGAZAT}:*GUS* gene also supports the assertion that HWS is necessary for cell separation to proceed at the normal rate.

Role of HWS in Plant Development

Although the principal characteristic of *hws-1* plants is their nonshedding phenotype, the isolation of a null allele (*hws*-2) of the gene has enabled us to dissect other consistent phenotypic features. A key difference from wild-type plants is that *hws-1* plants grown under the same environmental conditions have more elongated leaves and larger seeds. Plants ectopically expressing HWS exhibit a reduced overall stature compared to wild type with the degree of reduction being associated with the intensity of the up-regulation of the gene. These observations indicate that the target for HWS degradation plays a key role in the maintenance of organ growth. Indeed the impact of losing HWS can be seen in individual cells such as the stigmatic papillae where elongation is substantially elevated in the mutant and reduced in the overexpressing lines. A role for UFO in regulating organ growth has been previously identified (Laufs et al., 2003) and a number of F-box proteins have been linked to the regulation of the cell cycle (Taylor et al., 2001). Like UFO, HWS may have more than one direct role or perhaps may target more than one protein for degradation, alternatively, the consequence of HWS on sepal fusion might be mediated through its effects on the lateral expansion of sepal primordia, resulting in the generation of overlapping margins and a failure in organ separation. Intriguingly, silencing of *AUXIN RESPONSE FACTOR 2*, a transcription factor that mediates gene expression in response to auxin, also results in delayed floral organ abscission (Ellis et al., 2005) and increased growth of aerial organs and seeds (Schruff et al., 2006). Further work is ongoing to identify the mechanism by which HWS exerts its effect on growth and ascertain whether this may be mediated through an auxin-signaling pathway.

MATERIALS AND METHODS

Plant Material and Growth Conditions

Arabidopsis (*Arabidopsis thaliana*) ecotypes Col-0 and L*er*, the *hws-1* mutant, SALK lines for the 18 genes in the 56 kb segment that were obtained from the Nottingham Arabidopsis Stock Centre, diverse crosses, and the mapping population were grown in a glasshouse with a temperature of 23°C ± 2°C in plastic pots containing Levington M3 (The Scotts Company) compost and Vermiculite (2.0–5.0 mm, Sinclair) in a 3:1 ratio, respectively. To grow plants under sterile conditions, petri plates were prepared with 4.33 g L^{-1} of Murashige and Skoog basal salt mixture, pH 5.9 (Sigma; Murashige and

Skoog, 1962), and 0.8% agar or GM (Sedbrook et al., 2002); seeds were sterilized in a solution containing 50% (v/v) sodium hypochlorite then rinsed with a solution containing 0.01% (v/v) Triton X-100 for 5 min followed by ethanol (70% v/v). Seeds were then rinsed five times in sterile water before being placed, using a pipette tip, on top of the Murashige and Skoog agar petri dishes. Plates were sealed with micropore tape (3 M) and maintained at 4°C for 72 h to stratify them and to facilitate uniform germination. Plates were then transferred to a growth room with a temperature of 23°C ± 1°C under 16 h light/8 h dark.

The position of the flower was determined from the first site where petals were visible. From that position all subsequent flowers were numbered.

Scanning Electron Microscopy

Inflorescence apices and flowers were taken from Col-0 (wild type) and *hws-1* plants. Buds were staged in accord with Smyth et al. (1990) and flowers were harvested at inflorescence position 2, position 4, and position 14. The apex of the floral inflorescence was excised and placed directly into fixative (4% glutaraldehyde [w/v] in 0.5 M potassium phosphate buffer, pH 7.5) for 4 h prior to dehydration through a graded ethanol series and critical point drying in liquid CO_2. Specimens were then mounted on steel stubs with double-sided tape and dissected to reveal the floral primorida. They were sputter coated with gold palladium before viewing. Flowers were viewed immediately without fixation or sputter coating at 20 kV accelerating voltage in variable pressure mode under low vacuum (70 Pa). All samples were viewed under a Hitachi S-3000 SEM. A minimum of five buds/flower were examined from each position.

Light Microscopy

Unopened and open flowers were collected from wild type and the *hws-1* mutant when the plants were 1 month old. Young buds, mature buds, and flowers from positions 4, 6, 8, 12, 16, or 20 were fixed in 4% (v/v) paraformaldehyde: phosphate-buffered saline (PBS) buffer (1.3 mM NaCl, 0.03 M Na_2HPO_4, 0.03 M NaH_2PO_4, pH 7.2, 0.1% [v/v] Triton X-100, and 0.1% [v/v] Tween 20) overnight at 4°C. Tissues were washed with PBS at 4°C for 1 h, then brought to room temperature and washed with PBS for 1.5 h. The tissues were postfixed with 2% (w/v) OsO_4 in PBS at room temperature for 3 h, then rinsed twice in PBS for 15 min and dehydrated with an ethanol series (30%, 50%, 70%, 90%, and 100% [v/v], twice, for 1 h in each). Specimens were processed with 100% ethanol/propylene oxide (1:1) for 20 min, washed three times with propylene oxide for 10 min, and propylene oxide/Spurrs resin (1:1; TAAB) for 1.5 h. Specimens were infiltrated with pure Spurrs resin at 4°C for 10 to 12 h. Individual samples were placed in appropriate flat-labeled silicone embedding molds filled with Spurrs resin and placed at 72°C for 10 to 12 h.

Longitudinal semithin sections (0.5 μm) were cut on a Reichert-Jung Ultracut ultramicrotome using glass knives. The glass knives were made from a glass bar (TAAB) on a Leica EM KMR2 knife maker machine. Sections were stained with Toluidine blue (TBO) 0.25% to 1% (w/v), mounted with DePex (Sigma), and observed under a Nikon Optiphot-2 microscope equipped with a Leica DFC320 camera using the IM50 Leica software (Leica Microsystems Imaging Solutions).

Phenotypic and Statistical Analysis

Six plants from the *hws-1* mutant, wild type, and *35S* CaMV ectopic expression lines 8.3 or A23.3 were grown under the same conditions and 25 flowers were dissected and analyzed under a Zeiss Stemi SV6 Stereo microscope. Organ fusion and other phenotypic characteristics were recorded either with a Kodak MDS290 digital camera attached to the microscope or with a Fujifilm FinePix A205S. Images were analyzed with Adobe photoshop software.

Seedlings of 2 weeks old were grown in Murashige and Skoog media or in soil. Rosette leaves were dissected, and pictures taken with a Fujifilm FinePix A205S. For measurements of roots (26 plants grown in Murashige and Skoog media or GM media), the sepals, petals (12 flowers from different plants at position 3), and seeds (70 seeds from five plants) pictures were taken and measurements were performed with the image processor and analyzer in Java software ImageJ Version 1.37h (Abramoff et al., 2004). Values were then used to perform statistical analysis and create graphics in Microsoft Excel 2002. Statistical analysis of variance (one-way ANOVA) using LSD and Duncan Analysis were performed using the software SPSS 14.0.1.

Mapping of the *hws* Gene

A mapping population was generated by crossing the *hws-1* mutant in Col-0 background with the L*er* ecotype and the F_1 progeny was allowed to self. DNA was extracted, following manufacturer instructions (Qiagen, DNAeasy Plant Mini kit), from a small population of 33 F_2 *hws-1* mutant plants and used to map the *HWS* locus to a region of 3.28 MB between markers SM148,6 and SM239_119,5 at the bottom of chromosome 3 using an AFLP strategy as described by Peters et al. (2004).

With a further analysis of 156 *hws-1* mutant plants from the original F_2 population, using a combination of CAPS and SSLP, the region was reduced to a 0.404 MB between the markers FUS6.2 and NGA6. From 600 F_2 *hws-1* mutant plants, and the use of InDels that were identified from the Cereon Arabidopsis Polymorphism collection (Cereon Genomics; http://www.arabidopsis.org/Cereon/index.html), the region was further reduced to a segment of 56 kb between markers 470113 and 469675. This region contained 18 annotated genes (Fig. 5A). The InDel flanking primers designed for fine mapping *hws-1* are summarized in Supplemental Table S1. PCRs were performed in a reaction of 20 μL following red taq (ABgene) manufacturer instructions; the PCR conditions for amplification were: 3 min at 94°C, 30 cycles of 94°C for 30 s, 55°C to 60°C for 30 s (depending on primer combination), 72°C for 30 s, and 7 min at 72°C, 4°C ∞. PCR products were run in a 3% low melting point agarose gel (MetaPhor Agarose, Cambrex).

Salk KO lines were identified for the 18 annotated genes within this region and grown in the glasshouse. Individuals from one of these KO lines (Salk_088349), documented to contain a T-DNA insertion in *At3g61590*, proved to exhibit a similar phenotype to the *hws-1* mutant.

Primers from the region corresponding to the *At3g61590* gene that amplified a genomic PCR segment of 1,271 bp are At361590forcDNA: 5′GCTCTTGAGAATGGAAGCAGAAAC 3′ and At3g61590Rev: 5′CAGACCCATTTGCTTCTTCATTGC 3′. PCR reactions were performed in a 50 μL reaction following red taq (ABgene) manufacturer instructions. Conditions for amplification were: 3 min at 94°C, 30 cycles of 94°C for 15 s, 61°C for 1 min, 72°C for 2 min, 7 min at 72°C, 4°C, and the PCR products were run in a 1% agarose gel. The digestion of PCR products was performed in 20 μL reactions containing: 500 ng of PCR product, 10× reaction buffer, 2 μg of bovine serum albumin, and 0.5 μL of each enzyme, incubated at 37°C (*Rsa*I and *Alu*I) or 65°C (*Taq*I) and run in a 3% agarose gel. The expected restriction sizes for the amplified PCR segment corresponding to the *At3g61590* ORF genomic region are shown in Supplemental Table S2.

A plant from the Salk_088349 KO line was used to cross with the *hws-1* line and PCR analyses were performed to identify the presence of the two T-DNA insertions and the genomic fragment from the *hws-1* mutant from the two parental lines; information about primers is described previously. To test the T-DNA insertion the LBb1 of pBIN-pROK2 for SALK lines primer was used: 5′ GCGTGGACCGCTTGCTGCAACT 3′ (http://signal.salk.edu/tdnaprimers.2.html; Alonso et al., 2003). PCR conditions were the same as for the PCR amplification of the *At3g61590* segment described earlier.

RT-PCR Analysis of Expression

Total RNA from roots, buds, flowers, rosette leaves, stem, young siliques, and old siliques from wild type, and a mix of tissues from progeny plants 1 and 2 from the cross between the *hws-1* mutant with Salk_088349 line (*hws-2*) and from a mix of flowers from several developmental positions from F_1 overexpressing lines, was extracted using a modified method described by Han and Grierson (2002) where the removal of carbohydrates was performed by differential precipitation of RNA using 4 M LiCl at 20°C for 1 h instead of using the cetyl-trimethyl-ammonium bromide buffer. RNA was quantified with a spectrophotometer and its quality was analyzed by visualization in a 1% (w/v) agarose gel.

Expression analyses were determined using the SuperScript II Reverse Transcriptase kit from Invitrogen according to the manufacturer's instructions. First-strand cDNA synthesis was performed in a 20 μL reaction containing 2 μg of total RNA, 1 μL of 500 μg mL^{-1} oligo (dT), and 2 μL of 5 mM dNTPs and 13 μL of water.

PCR reactions were performed in 25 μL following red taq (ABgene) manufacturer instructions; the PCR conditions for amplification were: 3 min at 95°C, 30 cycles of 95°C for 1 min, 50°C to 58°C for 1 to 2 min (depending on primer combination and size of expected band), 72°C for 1 to 2 min, and 7 min at 72°C, 4°C. PCR products were run in a 1% agarose gel. The forward and reverse primers used in tissues from wild type, the progeny from crosses, and endogenous gene for overexpressing lines were 590 5′ UTR: 5′ CTTCTCTCATCCTCGCGCTTGCTCTCTC 3′ and At3g61590Rev (previously described)

that gave a genomic band of 2,213 bp and a cDNA of 1,668 bp. Use of these primers allows the identification of genomic contamination.

To amplify the transgene of overexpressing lines the primer pKT735Sprom 5′ GAGGAGCATCGTGGAAAAAG 3′ from the 35S promoter and At3g61590Rev were used. The amplified band from this primer combination is 1,677 bp.

Ubiquitin (At4g05320) primers UBQ10For, 5′-TAAAAACTTTCTCTCAATTCTCTCT-3′ and UBQ10Rev, 5′-AAGCTCCGACACCATTGACAA-3′ were used to evaluate the amounts of RNA levels in all tissues; these primers amplify a 1,555 bp from genomic DNA and 1,251 bp from cDNA; in addition, control reactions without reverse transcriptase were performed using the same conditions to confirm absence of genomic contamination in all RT-PCR reactions performed.

Plasmid Construction and Plant Transformation

All the constructs generated originated from wild-type genomic DNA extracted (Qiagen, DNAeasy Plant Mini kit) and amplified with the proof reading pfx DNA polymerase (Invitrogen) following the manufacturer's instructions. All the PCR products were subcloned in P-GEM T-Easy from Promega, unless otherwise specified, digested, and fused to the binary vectors at the multiple cloning site or at the site of digestion, as described below.

To perform the complementation test of the *hws-1* mutant, a genomic segment from *At3g61590* containing 1,291 bp of the promoter region, 419 bp from the 5′ UTR, 532 bp from the intron, 1,236 bp from the ORF, and 181 bp from the 3′ UTR using the primers 590compfor 5′ CCTCCAGTTTCAGAATCCGACC 3′and 590comprev 5′ CCTCCAGTTTCAGAATCCGACC 3′ was amplified from DNA of Col-0 wild type. Using this PCR product as template, the following primers containing a *Sal*I site and a *Bam*HI site in the forward and reverse primer, respectively (highlighted in bold), were used: 590CompSalFor, 5′ GCA**GTCGAC**GGCACTAAGGAGCAATGTG 3′ 590CompBamRev, 5′ GCC**GGATCC**TCCAGTTTCAGAATCCGAC 3′. The PCR parameters used were: 94°C for 5 min, followed by 35 cycles of 94°C for 15 s and 68°C for 3.5 min, and a final elongation step at 68°C for 7 min.

To generate the GUS reporter lines, a segment containing the promoter of the *HWS* (*At3g61590*), the 5′ UTR and the intron (2,242 bp), was also amplified by PCR. The primers used to amplify this genomic segment were the 590CompSalFor described previously and the 590PrBamRev 5′ GCC-**GGATCC**TCTCAAGAGCCTCTGAAAC 3′ with a *Sal*I and a *Bam*HI site at the forward and reverse primers, respectively (highlighted in bold). The PCR parameters used were: 94°C for 5 min, followed by 35 cycles of 94°C for 15 s and 68°C 2.5 min, and a final elongation step at 68°C for 7 min.

To generate the GFP lines, the Pro_{HWS}:*GUS* construct was modified by digesting and replacing the GUS gene with the *GFP* ORF also digested from the MOG vector used previously for the *PGAZAT* gene (González-Carranza et al., 2002). The enzymes used were *Bam*HI and *Sac*I (Fermentas) following manufacturer's instructions. Once the *HWS*::*GUS* construct was digested, the reaction was dephosphorylated with alkaline phosphatase (Promega) following the manufacturer's instructions. The digestions were visualized in a 1% agarose gel and the linearized/dephosphorylated vector and the *GFP* segment were gel extracted using a phenol:chloroform extraction method. The two segments were ligated using T4 DNA ligase from Promega following the manufacturer's instructions.

The overexpressor construct was generated by amplifying the ORF from the *HWS* gene using the primers: 59035SBamHATGfor, 5′ GCG**GGATCC**-CTCTTGAGAATGGAAGCAG 3′ and 59035SsacIrev, 5′ CGT**GAGCTC**C-CAGTTTCAGAATCCGACC 3′ with a *Bam*HI and a *Sac*I site at the forward and reverse primers, respectively (highlighted in bold). The PCR parameters used were the same as for the Pro_{HWS}:*GUS* construct. This segment was subcloned in a MOG402 engineered vector containing two copies of the *35S* CaMV promoter.

Escherichia coli DH5α cells were transformed and positive colonies were selected by PCR and the integrity of all plasmids generated was confirmed by sequencing, these plasmids were electroporated into *Agrobacterium tumefaciens* C58 strain and grown to an OD_{600} of 0.5 to 0.8. Wild-type Arabidopsis plants were transformed using the floral dip method described by Clough and Bent (1998).

Selection of transformants was carried out in a growth room at 22°C using petri dishes containing Murashige and Skoog media at pH 5.9, 0.8% (w/v) agar, and kanamycin 40 μg mL^{-1}. Transformation was confirmed by PCR using the correct set of primers per construct. For complementation tests, primary transformants were screened for kanamycin resistance and plants were grown and analyzed for rescue of the *hws* phenotype. T_2 seeds were collected from individual lines for the *GUS* and *GFP* reporter lines and the overexpressor lines, and screened for kanamycin resistance to identify at least six homozygous lines to check for consistency of expression.

Histochemical Analysis of GUS Activity

GUS staining, washing, and mounting for the different tissues analyzed was performed as described in González-Carranza et al. (2002). The material was analyzed and photographs taken using either a Zeiss Stemi SV6 Stereo microscope with a Kodak MDS290 digital camera or a Nikon microscope with a Leica DFC320 camera using the IM50 Leica software (Leica Microsystems Imaging Solutions).

Confocal Analyses of GFP Expression

GFP fluorescence in the transgenic lines was examined using a Leica (TCS SP2) laser-scanning confocal microscope equipped with argon krypton and green HeNe lasers and an AOBS scan head system (Leica Microsystems). GFP was excited at 488 nm with the argon ion laser. Images were recorded using the Leica CONFOCAL software.

Sequence data from this article can be found in the GenBank/EMBL data libraries under accession numbers BT000054/BX823146/BX824604 (At3g61590) and AAC02763 (At2g41850).

Supplemental Data

The following materials are available in the online version of this article.

Supplemental Figure S1. Analysis of expression from Pro_{35S}:*HWS* lines by RT-PCR.

Supplemental Figure S2. Comparative phenotypic analysis of flowers at position 9.

Supplemental Figure S3. Comparative phenotypic analysis of sepals and petals.

Supplemental Table S1. InDel primers used for mapping the *HWS* locus through the identification of Col/L*er* polymorphisms.

Supplemental Table S2. Restriction enzymes and expected sizes for the digestion of the PCR product corresponding to the *At3g61590* ORF genomic region.

ACKNOWLEDGMENTS

We thank Rick Noteboom (Radboud University, Nijmegen, The Netherlands) for technical help in the map-based cloning experiments and Patricia Goggin of the Electron Microscopy Unit at Royal Holloway.

Received October 31, 2006; accepted April 29, 2007; published May 11, 2007.

LITERATURE CITED

Abramoff MD, Magelhaes PJ, Ram SJ (2004) Image processing with ImageJ. J Biophotonics Int **11:** 36–42

Addicott FT (1982) Abscission. University of California Press, Berkeley, CA

Aida M, Ishida T, Fukaki H, Fujishawa H, Tasaka M (1997) Genes involved in organ separation in Arabidopsis: an analysis of the *cuc-shaped cotyledon* mutant. Plant Cell **9:** 841–857

Alonso JM, Stepanova AN, Leisse TJ, Kim CJ, Chen H, Shinn P, Stevenson DK, Zimmerman J, Barajas P, Cheuk R, et al (2003) Genome-wide insertional mutagenesis of *Arabidopsis thaliana.* Science **301:** 653–657

Belfield EJ, Ruperti B, Roberts JA, McQueen-Mason S (2005) Changes in expansin activity and gene expression during ethylene-promoted leaflet abscission in *Sambucus nigra.* J Exp Bot **56:** 817–823

Brewer P, Howles P, Dorian K, Griffith M, Ishida T, Kaplan-Levy R, Kilinc A, Smyth D (2004) Petal loss, a trihelix transcription factor gene, regulates perianth architecture in the Arabidopsis flower. Development **131:** 4035–4045

Butenko MA, Patterson SE, Grini PE, Stenvik G-E, Amundsen SS, Mandal A, Aalen RB (2003) *INFLORESCENCE DEFICIENT IN ABSCISSION* controls floral organ abscission in Arabidopsis and identifies a novel family of putative ligands in plants. Plant Cell **15:** 2296–2307

Clough SJ, Bent AF (1998) Floral dip: a simplified method for *Agrobacterium*-mediated transformation of *Arabidopsis thaliana*. Plant J **16:** 735–743

Durfee T, Roe JL, Sessions RA, Inouye C, Serikawa K, Feldmann KA, Weigel D, Zambryski PC (2003) The F-box-containing protein UFO and AGAMOUS participate in antagonistic pathways governing early petal development in Arabidopsis. Proc Natl Acad Sci USA **100:** 8571–8576

Ellis CM, Nagpal P, Young JC, Hagen G, Guilfoyle TJ, Reed JW (2005) *AUXIN RESPONSE FACTOR1* and *AUXIN RESPONSE FACTOR2* regulate senescence and floral organ abscission in *Arabidopsis*. Development **132:** 4563–4574

Fernandez DE, Heck GR, Perry SE, Patterson SE, Bleecker AB, Fang S-C (2000) The embryo MADS domain factor AGL15 acts postembryonically: inhibition of perianth senescence and abscission via constitutive expression. Plant Cell **12:** 183–198

González-Carranza ZH, Lozoya-Gloria E, Roberts JA (1998) Recent developments in abscission: shedding light on the shedding process. Trends Plant Sci **3:** 10–14

González-Carranza ZH, Whitelaw CA, Swarup R, Roberts JA (2002) Temporal and spatial expression of a polygalacturonase during leaf and flower abscission in oilseed rape and Arabidopsis. Plant Physiol **128:** 534–543

Gray WM, del Pozo CJ, Walker L, Hobbie L, Risseeuw E, Banks T, Crosby WL, Yang M, Ma H, Estelle M (1999) Identification of an SCF ubiquitin-ligase complex required for auxin response in *Arabidopsis thaliana*. Genes Dev **13:** 1678–1691

Han Y, Grierson D (2002) Relationship between small antisense RNAs and aberrant RNAs associated with sense transgene mediated gene silencing in tomato. Plant J **29:** 509–519

Harding EW, Tang W, Nichols KW, Fernandez DE, Perry SE (2003) Expression and maintenance of embryogenic potential is enhanced through constitutive expression of *AGAMOUS-Like 15*. Plant Physiol **133:** 653–663

Hepworth SR, Zhang Y, McKim S, Li X, Haughn GW (2005) *BLADE-ON-PETIOLE1* dependent signaling controls leaf and floral patterning in Arabidopsis. Plant Cell **17:** 1434–1448

Jarillo JA, Capel J, Tang RH, Yang HQ, Alonso JM, Ecker JR, Cashmore AR (2001) An *Arabidopsis* circadian clock component interacts with both CRY1 and phyB. Nature **410:** 487–490

Jinn T-L, Stone JM, Walker JC (2000) *HAESA*, an *Arabidopsis* leucine-rich repeat receptor kinase, controls floral organ abscission. Genes Dev **14:** 108–117

Kepinski S, Leyser O (2005) The *Arabidopisis* F-box protein TIR1 is an auxin receptor. Nature **435:** 446–451

Krizek BA, Lewis MW, Fletcher JC (2006) *RABBIT EARS* is a second-world repressor of *AGAMOUS* that maintains spatial boundaries in Arabidopsis flowers. Plant J **45:** 369–383

Laufs P, Coen E, Kronenberger J, Traas J, Doonan J (2003) Separable roles of *UFO* during floral development revealed by conditional restoration of gene function. Development **130:** 785–796

Laufs P, Peaucelle A, Morin H, Traas J (2004) MicroRNA regulation of the CUC genes is required for boundary size control in *Arabidopsis* meristems. Development **131:** 4311–4322

Lehti-Shiu MD, Adamczyk BJ, Fernandez DE (2005) Expression of MADS-box genes during the embryonic phase in *Arabidopsis*. Plant Mol Biol **58:** 89–107

Levin J, Fletcher J, Chen X, Meyerowitz E (1998) A genetic screen for modifiers of UFO meristem activity identifies three novel fused floral organs genes required for early flower development in *Arabidopsis*. Genetics **149:** 579–595

Levin JZ, Meyerowitz EM (1995) *UFO*: an Arabidopsis gene involved in both floral meristem and floral organ development. Plant Cell **7:** 529–548

Li C, Zhou A, Sang T (2006) Rice domestication by reducing shattering. Science **311:** 1936–1939

Mallory AC, Dugas DV, Bartel DP, Bartel B (2004) MicroRNA regulation of NAC-domain targets is required for proper formation and separation of adjacent embryonic, vegetative, and floral organs. Curr Biol **14:** 1035–1046

Mao L, Begum D, Chuang HW, Budiman MA, Szymkowiak EJ, Irish EE, Wing RA (2000) *JOINTLESS* is a MADS-box gene controlling tomato flower abscission zone development. Nature **406:** 910–913

Murashige T, Skoog F (1962) A revised medium for rapid growth and bioassays with tobacco tissue cultures. Physiol Plant **18:** 100–127

Ni W, Xie D, Hobbie L, Feng B, Zhao D, Akkara J, Ma H (2004) Regulation of flower development in Arabidopsis by SCF complexes. Plant Physiol **134:** 1574–1585

Norberg M, Holmlund M, Nilsson O (2005) The *BLADE ON PETIOLE* genes act redundantly to control growth and development of lateral organs. Development **132:** 2203–2213

Patterson SE (2001) Cutting loose: abscission and dehiscence in Arabidopsis. Plant Physiol **126:** 494–500

Peters JL, Cnops G, Neyt P, Zethof J, Cornelis K, Van Lijsebettens M, Gerats T (2004) An AFLP-based genome-wide mapping strategy. Theor Appl Genet **108:** 321–327

Prasad AM, Sivanandan C, Resminath R, Thakare DR, Bhat SR, Srinivasan (2005) Cloning and characterization of a pentatricopeptide protein encoding gene (*LOJ*) that is specifically expressed in lateral organ junctions in *Arabidopsis thaliana*. Gene **353:** 67–79

Roberts JA, Elliott KA, González-Carranza ZH (2002) Abscission, dehiscence, and other cell separation processes. Annu Rev Plant Biol **53:** 131–158

Samach A, Klenz JE, Kohalmi SE, Risseeuw E, Haughn GW, Crosby WL (1999) The *UNUSUAL FLORAL ORGANS* gene of *Arabidopsis thaliana* is an F-box protein required for normal patterning and growth in the floral meristem. Plant J **20:** 433–445

Sampedro J, Cosgrove DJ (2005) The expansin superfamily. Genome Biol **6:** 242

Schruff MC, Spielman M, Tiwari S, Adams S, Fenby N, Scott RJ (2006) The *AUXIN RESPONSE FACTOR2* gene of *Arabidopsis* links auxin signalling, cell division, and the size of seeds and other organs. Development **133:** 251–261

Schultz EA, Haughn GW (1991) LEAFY, a homeotic gene that regulates inflorescence development in Arabidopsis. Plant Cell **3:** 771–781

Sedbrook JC, Carroll KL, Hing KF, Masson PH, Somerville CR (2002) The Arabidopsis *SKU5* gene encodes an extracellular glycosyl phosphatidylinositol-anchored glycoprotein involved in directional root growth. Plant Cell **14:** 1635–1648

Sexton R, Roberts JA (1982) Cell biology of abscission. Annu Rev Plant Physiol **33:** 133–162

Shuai B, Reynaga-Peña CG, Springer PS (2002) The *LATERAL ORGAN BOUNDARIES* gene defines a novel, plant-specific gene family. Plant Physiol **129:** 747–761

Smyth DR, Bowman JL, Meyerowitz EM (1990) Early flower development in Arabidopsis. Plant Cell **2:** 755–767

Stenvik G-E, Butenko MA, Urbanowicz BR, Rose JKC, Aalen RB (2006) Overexpression of INFLORESENCE DEFICIENT IN ABSCISSION activates cell separation in vestigial abscission zones in Arabidopsis. Plant Cell **18:** 1467–1476

Takada S, Hibara K, Ishida T, Tasaka M (2001) The *CUP-SHAPED COTYLEDON1* gene of *Arabidopsis thaliana* regulates shoot apical meristem formation. Development **128:** 1127–1135

Takahashi N, Kuroda H, Kuromori T, Hirayama T, Seki M, Shinozaki K, Shimada H, Matsui M (2004) Expression and interaction analysis of *Arabidopsis Skp1*-related genes. Plant Cell Physiol **45:** 83–91

Taylor JE, Whitelaw CA (2001) Signals in abscission. New Phytol **151:** 323–339

Taylor S, Hofer J, Murfet I (2001) *Stamina pistilloida*, the pea orthologue of *Fim* and *UFO*, is required for normal development of flowers, inflorescences, and leaves. Plant Cell **13:** 31–46

Vroemen CW, Mordhorst AP, Albretch C, Kwaaitaal CJ, de Vries SC (2003) The *CUC-SHAPED COTYLEDON3* gene is required for boundary and shoot meristem formation in Arabidopsis. Plant Cell **15:** 1563–1577

Weigel D, Meyerowitz EM (1993) Activation of floral homeotic genes in *Arabidopsis*. Science **261:** 1723–1726

Zhao Y, Medrano L, Ohasho K, Fletcher JC, Yu H, Sakai H, Meyerowitz EM (2004) HANABA TARANU is a GATA transcription factor that regulates shoot apical meristem and flower development in Arabidopsis. Plant Cell **16:** 2586–2600